Strangeness and hypernuclear production in fragmentation reactions induced by antikaons

Zhao-Qing Feng*
School of Physics and Optoelectronics, South China University of Technology, Guangzhou 510640, China

(Received 16 October 2019; published 10 January 2020)

The formation mechanism of hyperfragments with strangeness $s = -1$ and $s = -2$ in collisions of antikaons on nuclei has been investigated within a microscopic transport model. Dynamics of pseudoscalar mesons and hyperons is modeled within the transport model, in which all possible reaction channels for creating hyperons such as the elastic scattering, resonance production and decay, strangeness exchange reaction, and direct strangeness production in meson-baryon and baryon-baryon collisions have been included. A coalescence approach is used for constructing hyperfragments in phase space and the statistical model is modified to describe the decay of hyperfragments. It is found that the Ξ^- production is correlated to the K^+ dynamics. The hyperons Λ and Σ are created within a broad rapidity region. The production cross sections of nucleonic fragments and hyperfragments weakly depends on the incident momentum. The yields of Λ hyperfragments are the sixth order of magnitude of Ξ^- hyperfragments. Possible experiments on the hypernuclear physics at the high-intensity heavy-ion accelerator facility (HIAF) in China are discussed.

DOI: 10.1103/PhysRevC.101.014605

I. INTRODUCTION

Inclusion of the strangeness degree of freedom in the nuclear medium extends the research activities in nuclear physics, in particular regarding the issues of the nuclear structure of the hypernucleus and kaonic nucleus, hyperon-nucleon and hyperon-hyperon interactions, and probing the in-medium properties of hadrons [1–4]. Moreover, hadrons with strangeness as an essential ingredient influence the high-density nuclear equation of state (EOS). The strangeness ingredient in dense matter softens the EoS at high baryon densities, and consequently decreases the mass of neutron stars [5,6]. Since the first observation of the Λ hypernuclide in nuclear multifragmentation reactions induced by cosmic rays in the 1950s [7], remarkable progress has been made in producing hypernuclides via different reaction mechanisms, such as hadron (pion, $K^{\pm}$, proton, antiproton) induced reactions, bombarding the atomic nucleus with high-energy photons or electrons, and fragmentation reactions with high-energy heavy-ion collisions. Experimental collaborations of nuclear physics facilities have started or planned investigating hypernuclei and their properties, e.g., PANDA [8], FOPI/CBM and Super-FRS/NUSTAR [9] at FAIR (GSI, Germany), STAR at RHIC (BNL,USA) [10], ALICE at LHC (CERN) [11], NICA (Dubna, Russia) [12], J-PARC (Japan) [13], and HIAF (IMP, China) [14]. In these laboratories, the strangeness nuclear physics research will concentrate on the isospin degree of freedom (neutron-rich/proton-rich hypernuclei), multiple strangeness nuclei, antihypernuclei, and high-density hadronic matter with strangeness. Hypernuclear spectroscopy and kinematics in antikaon induced reactions have been investigated in experiments [15,16]. A theoretical description of hypernucleus formation is helpful for managing the detector systems in experiments.

The dynamics mechanism of hypernucleus formation in antikaon induced reactions is a complex process and is related to the creation of hyperons, propagation, and hyperfragment construction and decay. Up to now, several models have been established for describing the hypernucleus formation in nuclear reactions, i.e., the statistical multifragmentation model (SMM) [17,18], a statistical approach with a thermal source [19], and microscopic transport models based on the Boltzmann-Uheling-Uhlenbeck (BUU) model and quantum molecular dynamics (QMD) [20–23]. Some interesting results are obtained toward understanding hypernucleus production, i.e., the yields of hyperfragments, fragment production with multiple strangeness, dibaryon states, etc.

In this work, the strangeness production and hypernuclear dynamics in antikaon induced reactions are to be investigated within the Lanzhou quantum molecular dynamics (LQMD) transport model. The article is organized as follows. In Sec. II I give a brief description of the model. The calculated results and discussion are presented in Sec. III. A Summary and perspective on hypernuclear physics are outlined in Sec. IV.

II. BRIEF DESCRIPTION OF THE LQMD MODEL

In the model, the dynamics of resonances [$\Delta(1232)$, $N^*(1440)$, $N^*(1535)$, etc.], hyperons (Λ, Σ, Ξ), and mesons ($\pi, K, \eta, \overline{K}, \rho, \omega$) is included and coupled to the reaction channels via hadron-hadron collisions and decay of resonances [24,25]. The evolutions of hadrons in nuclear medium are described by Hamilton's equations of motion under the self-consistently generated mean-field potentials. The Hamiltonian

*fengzhq@scut.edu.cn

of mesons and hyperons is constructed as follows:

$$H = \sum_{i=1}^{N_H} \left[V_i^{\rm Coul} + \omega(\mathbf{p}_i, \rho_i) \right]. \quad (1)$$

Here, N_P is the total number of mesons or hyperons. The hyperon mean-field potential is constructed on the basis of the light-quark counting rule. The self-energies of Λ and Σ are assumed to be two-thirds of that experienced by nucleons, and the Ξ self-energy is one third of the nucleons'. Thus, the in-medium dispersion relation reads

$$\omega(\mathbf{p}_i, \rho_i) = \sqrt{\left(m_Y + \Sigma_S^Y\right)^2 + \mathbf{p}_i^2} + \Sigma_V^Y, \quad (2)$$

e.g., for hyperons $\Sigma_S^{\Lambda,\Sigma} = 2\Sigma_S^N/3$, $\Sigma_V^{\Lambda,\Sigma} = 2\Sigma_V^N/3$, $\Sigma_S^{\Xi} = \Sigma_S^N/3$, and $\Sigma_V^{\Xi} = \Sigma_V^N/3$. The nucleon scalar Σ_S^N and vector Σ_V^N self-energies are computed from the well-known relativistic mean-field model with the NL3 parameter ($g_{\sigma N} = 8.99$, $g_{\omega N} = 12.45$, and $g_{\rho N} = 4.47$) [26]. The optical potential of hyperon is derived from the in-medium energy as $V_{\rm opt}(\mathbf{p}, \rho) = \omega_Y(\mathbf{p}, \rho) - \sqrt{\mathbf{p}^2 + m^2}$. The values of optical potentials at saturation density are -32 and -16 MeV for $\Lambda(\Sigma)$ and Ξ, respectively. The attractive potential is available for the bound hyperfragment formation. The in-medium effects of pseudoscalar mesons (π, η, K, and $\overline{K}$) in heavy-ion collisions have been investigated and the optical potentials at the saturation density have been extracted [25,27]. The kaon and antikaon energies in the nuclear medium are calculated with the chiral Lagrangian approach [28], in which the isospin effect and Lorentz force are implemented in the propagation [29].

In the K^- induced reactions, hyperons are mainly created via the strangeness exchange reaction of $K^-N \to \pi Y$ and the direct channel of $K^-N \to K^+\Xi$. The cross section of $K^-N \to \pi Y$ is implemented by fitting the available experimental data [25]. The in-medium cross section is corrected by the threshold energy. The effective mass is used to evaluate the threshold energy, e.g., the threshold energy in the antikaon-nucleon collisions, $\sqrt{s} = m_Y^* + m_\pi^*$. The Ξ production is estimated by a parametrized formula [30], which is basically consistent with the calculations by a phenomenological model [31]. The isotropic distribution of hyperon is assumed once it created. The yields of Λ and Σ are abundant because of larger cross sections. The production rate of Ξ is very low, but it can be easily captured by nucleonic fragments to form hyperfragments owing to the low relative momentum.

III. RESULTS AND DISCUSSION

The target nuclide can be heated by an incoming energetic antikaon, which leads to the fragmentation reaction. The primary fragments are constructed in phase space with a coalescence model, in which nucleons at freeze-out are considered to belong to one cluster with relative momentum smaller than P_0 and with relative distance smaller than R_0 (here $P_0 = 200$ MeV/c and $R_0 = 3$ fm). The hyperons are captured by nucleonic fragments to form Λ fragments. Here, there is a larger relative distance ($R_0 = 5$ fm) and the relative momentum is similar to nucleonic ones ($P_0 = 200$ MeV/c) between hyperon and nucleon in constructing a hypernucleus, owing to the more weakly bound hypernucleus with a bigger rms (root-mean-square) radius, e.g., 5 fm rms for ${}^{3}_{\Lambda}$H and 1.74 fm for ^{3}He [32]. At freeze-out, the primary hyperfragments are highly excited. The deexcitation of the hyperfragments is described within the GEMINI code [33], in which the decay width of light fragments with $Z \leqslant 2$ and the binary decay are calculated by the Hauser-Feshbach formalism [34] and transition state formalism [35], respectively. I implemented the hyperon decay based on the Hauser-Feshbach approach. The binding energy of the hyperon is evaluated by a phenomenological formula [36]. Shown in Fig. 1 are the decay widths of neutron, proton, α, Λ, and fission from excited ${}^{40}_{\Lambda}$Ca and ${}^{238}_{\Lambda}$U. The Λ emission is the dominant decay mode for the light nucleus because of the small separation energy. Neutron evaporation and binary fission are competitive for the heavy nucleus.

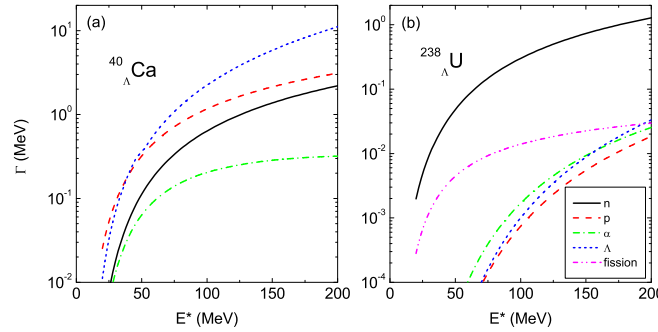

FIG. 1. Decay widths for evaporating neutron, proton, α, and Λ and fission of ${}^{40}_{\Lambda}$Ca and ${}^{238}_{\Lambda}$U as a function excitation energy.

The emission mechanism of particles produced in antikaon induced reactions is significant for understanding contributions of different reaction channels associated with antikaons on nucleons and secondary collisions. Shown in Fig. 2 are the excitation functions of π, η, K^+, Λ, Σ, and Ξ^- in the reaction of K^- + ^{40}Ca. It is obvious that the π and hyperons (Λ, Σ) slightly decrease with the beam momentum. The K^+ and Ξ^- can be created above the threshold energy ($p_{th} = 1.04$ GeV/c) and the yields increase rapidly with the momentum. Once a low-momentum hyperon is created, it can be easily captured by the potential well to form hyperfragments. Both the

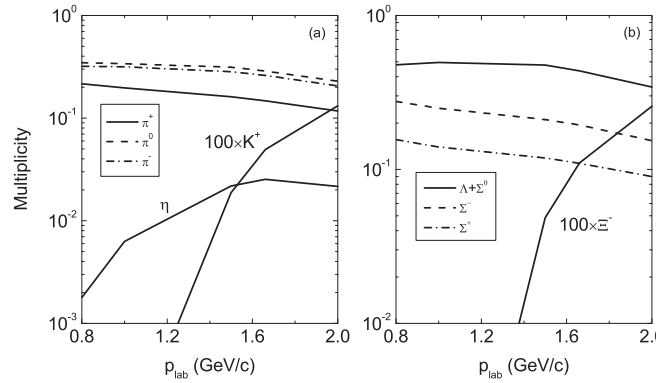

FIG. 2. Production of mesons and hyperons in K^- induced reactions on ^{40}Ca as a function of beam momentum.

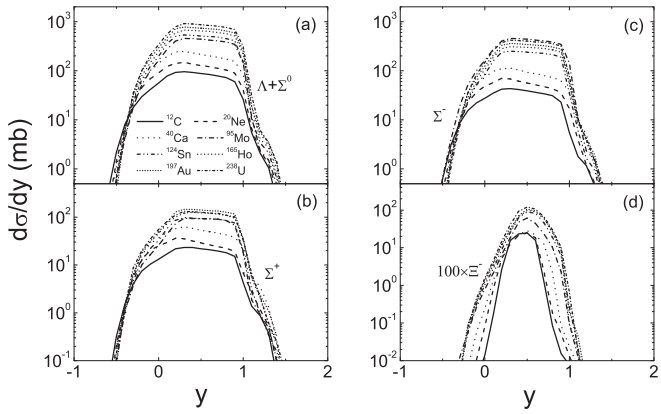

FIG. 3. Rapidity distributions of free hyperons in collisions of K^- on ^{12}C, ^{20}Ne, ^{40}Ca, ^{95}Mo, ^{124}Sn, ^{165}Ho, ^{197}Au, and ^{238}U at incident momentum 1.5 GeV/c.

abundance and phase-space distribution of produced hyperons contribute the production rate of hypernuclides.

The hyperon production in heavy-ion collisions near threshold energies has been investigated extensively in experiments and in theories, in particular regarding the issues of nuclear equation of state, hyperon-nucleon interaction, correlation of hyperon production, etc. [37–42]. The hyperon distribution in phase space dominates the hypernuclear formation in antikaon induced reactions. Shown in Fig. 3 are the rapidity distributions of hyperons produced in the reactions of K^- on ^{12}C, ^{20}Ne, ^{40}Ca, ^{95}Mo, ^{124}Sn, ^{165}Ho, ^{197}Au, and ^{238}U at incident momentum 1.5 GeV/c. A broad structure is obvious for the production of Λ and Σ with enough cross sections. The Ξ^- yields are strongly reduced with narrow shape. The invariant spectra of particle production manifest hadronic matter properties. I calculated the kinetic energy spectra of π^-, K^+, $\Lambda + \Sigma^0$, and Ξ^- as shown in Fig. 4. A steep structure is pronounced for the K^+ production. The reabsorption process by surrounding nucleons retards the particle emission and leads to a platform in the energy spectra.

The study of nuclear dynamics induced by antikaons is motivated by the aspects of strangeness exchange reactions,

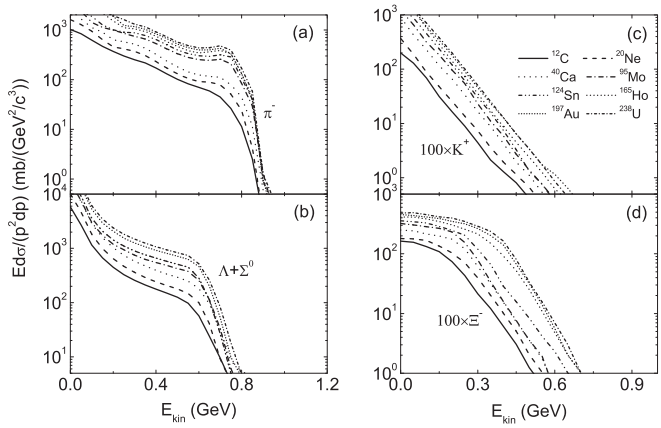

FIG. 4. Inclusive spectra of π^-, K^+, $\Lambda + \Sigma^0$, and Ξ^- in K^- induced reactions on different target nuclei at momentum 1.5 GeV/c.

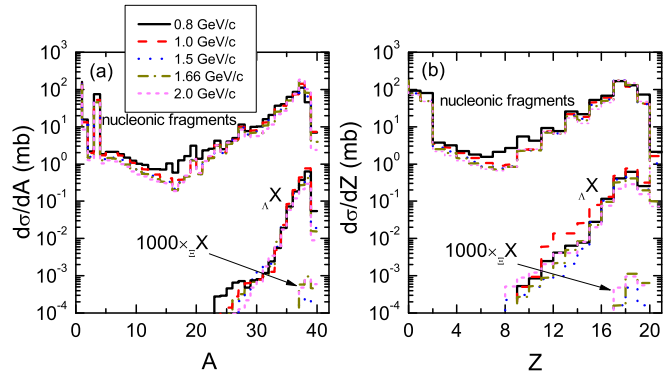

FIG. 5. Incident energy dependence of the nucleonic fragments, Λ hyperfragments, and Ξ^- hyperfragments as functions of mass and charge numbers in collisions of $K^- + {}^{40}$Ca, respectively.

nuclear fragmentation, liquid-gas phase transition, hypernuclide formation, etc. On the other hand, antikaon-nucleus collisions have advantages for investigating the energy dissipation mechanism, the interaction of strange particles and nucleons, and hadronic matter properties around the saturation density. Shown in Fig. 5 is a comparison of the nucleonic fragments, Λ hyperfragments, and Ξ^- hyperfragments in the $K^- + {}^{40}$Ca reaction at different incident momenta. The strangeness exchange reaction $K^-N \to \pi Y$ dominates the hyperon production. Once the Λ is created in the nucleus, there is a large probability of capture to form a hypernucleus. The nucleonic fragments are mainly produced in the target-like region and the light clusters are from the decay of excited fragments. The fragmentation in the antikaon induced reactions weakly depends on the incident energy. The production of Λ hyperfragments is roughly the sixth order of magnitude of the Ξ^- hypernuclear yields. The hypernuclear fragments in the antikaon induced reactions are formed in the domain of target-like fragments. The production cross sections are measurable in experiments: i.e., the Λ hypernuclide with a magnitude of mb and the double strangeness hypernuclear formation at the level of nb. The mass and charge spectra of nucleonic fragments and hyperfragments in the fragmentation reaction on ^{95}Mo are calculated as shown in Fig. 6. The hypernuclear

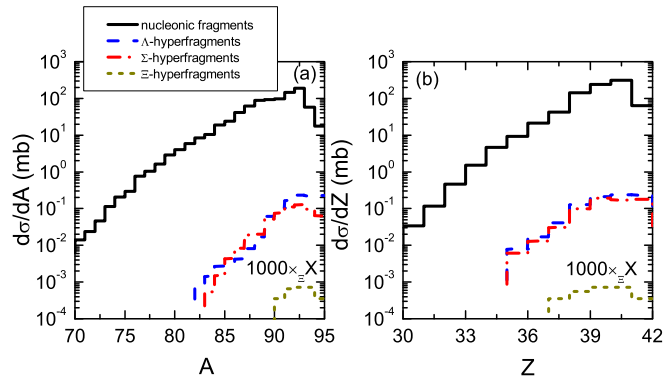

FIG. 6. Comparison of nucleonic fragments and Λ, Σ, and Ξ^- hyperfragments in K^- induced reactions on ^{95}Mo at incident momentum 1.5 GeV/c.

production is reduced to the third order of magnitude of nucleonic fragments. It should be noticed that the production cross sections of double strangeness hyperfragments are low in comparison to the ones in the antiproton [21] or Ξ^- induced reactions [43]. The results will be helpful for hypernuclear physics with high-intensity antikaon beams at J-PARC and HIAF in the near future.

IV. CONCLUSIONS

In summary, the particle production in K^- induced reactions has been investigated within the LQMD transport model. The π, Λ, and Σ are mainly created from strangeness exchange reactions and weakly depend on the beam momentum. However, the abundance of K^+ and Ξ^- increases rapidly with the incident momentum. Broad rapidity and transverse momentum spectra are obtained for Λ and Σ production, which enable the formation of hyperfragments. The target nucleus is heated by K^--nucleon collisions and fragmentation takes place in the target-like region. The double-strangeness hypernuclides in K^- induced reactions are formed with cross sections at the level of nb, and are independent of the incident momentum above the threshold energy of Ξ^- production. Measurements will be feasible at J-PARC and HIAF in the near future.

ACKNOWLEDGMENTS

This work was supported by the National Natural Science Foundation of China (Projects No. 11722546 and No. 11675226) and the Talent Program of South China University of Technology.

[1] B. E. Gibson and E. V. Hungerford III, Phys. Rep. **257**, 349 (1995).
[2] T. Falter, J. Lehr, U. Mosel, P. Muehlich, and M. Post, Prog. Part. Nucl. Phys. **53**, 25 (2004).
[3] O. Hashimoto and H. Tamura, Prog. Part. Nucl. Phys. **57**, 564 (2006).
[4] H. Lenske and M. Dhar, in *The Euroschool on Exotic Beams - Vol. 5*, Lecture Notes in Physics Vol. 948 (Springer, Cham, 2018), p. 161; H. Lenske, M. Dhar, T. Gaitanos, and X. Cao, Prog. Part. Nucl. Phys. **98**, 119 (2018).
[5] W. Z. Jiang, R. Y. Yang, and D. R. Zhang, Phys. Rev. C **87**, 064314 (2013).
[6] S. Weissenborn, D. Chatterjee, and J. Schaffner-Bielich, Nucl. Phys. A **881**, 62 (2012).
[7] M. Danysz and J. Pniewski, Philos. Mag. **44**, 348 (1953).
[8] PANDA Collaboration, http://www-panda.gsi.de, K.-T. Brinkmann, P. Gianotti, and I. Lehmann, Nucl. Phys. News **16**, 15 (2006).
[9] T. R. Saito, D. Nakajima, C. Rappold *et al.*, Nucl. Phys. A **881**, 218 (2012); T. R. Saito, E. Kim, and D. Nakajima, Few-Body Syst. **54**, 1211 (2013).
[10] STAR Collaboration, Science **328**, 58 (2010).
[11] B. Dönigus *et al.* (ALICE Collaboration), Nucl. Phys. A **904-905**, 547c (2013).
[12] NICA White Paper, http://theor.jinr.ru/twiki-cgi/view/NICA/WebHome.
[13] H. Tamura, Prog. Theor. Exp. Phys. **2012**, 02B012 (2012).
[14] J. C. Yang, J. W. Xia, G. Q. Xiao *et al.*, Nucl. Instrum. Methods B **317**, 263 (2013).
[15] K. Nakazawa, S. Kinbara, A. Mishina *et al.*, J. Phys. G: Conf. Series **569**, 012082 (2014).
[16] A. Gal, E. V. Hungerford, and D. J. Millener, Rev. Mod. Phys. **88**, 035004 (2016).
[17] A. S. Botvina and J. Pochodzalla, Phys. Rev. C **76**, 024909 (2007); A. S. Botvina, K. K. Gudima, J. Steinheimer *et al.*, Nucl. Phys. A **881**, 228 (2012).
[18] S. Bleser *et al.*, Phys. Lett. B **790**, 502 (2019).
[19] A. Andronic, P. Braun-Munzinger, J. Stachel, and H. Stöcker, Phys. Lett. B **697**, 203 (2011).
[20] A. S. Botvina, J. Steinheimer, E. Bratkovskaya, M. Bleicher, and J. Pochodzalla, Phys. Lett. B **742**, 7 (2015).
[21] Z. Q. Feng, Phys. Rev. C **93**, 041601(R) (2016).
[22] T. Gaitanos, Ch. Moustakidis, G. A. Lalazissis, and H. Lenske, Nucl. Phys. A **954**, 308 (2016).
[23] A. Le Fèvre, J. Aichelin, C. Hartnack, and Y. Leifels, Phys. Rev. C **100**, 034904 (2019).
[24] Z. Q. Feng, Phys. Rev. C **84**, 024610 (2011); **85**, 014604 (2012).
[25] Z. Q. Feng, Nucl. Sci. Technol. **29**, 40 (2018).
[26] G. A. Lalazissis, J. König, and P. Ring, Phys. Rev. C **55**, 540 (1997).
[27] Z. Q. Feng, W. J. Xie, P. H. Chen, J. Chen, and G. M. Jin, Phys. Rev. C **92**, 044604 (2015).
[28] D. B. Kaplan and A. E. Nelson, Phys. Lett. B **175**, 57 (1986).
[29] Z. Q. Feng, Nucl. Phys. A **919**, 32 (2013).
[30] F. Li, L. W. Chen, C. M. Ko, and S. H. Lee, Phys. Rev. C **85**, 064902 (2012).
[31] D. A. Sharov, V. L. Krotkikh, and D. E. Lanskoy, Eur. Phys. J. A **47**, 109 (2011).
[32] T. A. Armstrong *et al.*, Phys. Rev. C **70**, 024902 (2004).
[33] R. J. Charity *et al.*, Nucl. Phys. A **483**, 371 (1988).
[34] H. Hauser and H. Feshbach, Phys. Rev. **87**, 366 (1952).
[35] L. G. Moretto, Nucl. Phys. A **247**, 211 (1975).
[36] C. Samanta, P. Roy Chowdhury, and D. N. Basu, J. Phys. G: Nucl. Part. Phys. **32**, 363 (2006).
[37] C. Sturm *et al.* (KaoS Collaboration), Phys. Rev. Lett. **86**, 39 (2001).
[38] Y. M. Zheng, C. Fuchs, A. Faessler, K. Shekhter, Y. P. Yan, and C. Kobdaj, Phys. Rev. C **69**, 034907 (2004).
[39] C. Hartnack, H. Oeschler, Y. Leifels, E. Bratkovskaya, and J. Aichelin, Phys. Rep. **510**, 119 (2012).
[40] A. B. Larionov, T. Gaitanos, and U. Mosel, Phys. Rev. C **85**, 024614 (2012).
[41] O. Buss *et al.*, Phys. Rep. **512**, 1 (2012).
[42] Z. Q. Feng, W. J. Xie, and G. M. Jin, Phys. Rev. C **90**, 064604 (2014).
[43] T. Gaitanos and H. Lenske, Phys. Lett. B **737**, 256 (2014).